Journal of Molecular Spectroscopy 368 (2020) 111257

Contents lists available at ScienceDirect

Journal of Molecular Spectroscopy

journal homepage: www.elsevier.com/locate/jms

Continuous temporal ion detection combined with time-gated imaging: Normalization over a large dynamic range

Yuval Shagam *, William B. Cairncross [1], Tanya S. Roussy, Yan Zhou [2], Kia Boon Ng, Daniel N. Gresh [3], Tanner Grogan, Jun Ye, Eric A. Cornell

JILA, NIST and the University of Colorado, and the Department of Physics, University of Colorado, Boulder, CO 80309-0440, USA

ARTICLE INFO

Article history:
Received 16 September 2019
In revised form 7 January 2020
Accepted 9 February 2020
Available online 15 February 2020

Keywords:
Phosphor
Micro-channel plate
Imaging

ABSTRACT

Imaging micro-channel plate (MCP) detectors are a common tool for chemical physics studies used to image a single ion mass species in a time-of-flight (TOF) spectrum. Temporal selection of the mass to be imaged is traditionally implemented by gating the voltage across the MCP stack, however this leads to the loss of all information about other species in the mass spectrum. Here we show that by gating the phosphor voltage instead, as has been demonstrated by Zajfman et al. (1995) among others, we gain the capability of measuring multiple masses in TOF while retaining the ability to image a single desired species. In our precision spectroscopy experiment, we image the spatial distribution of Hf^+ photodissociation fragments, while its more plentiful HfF^+ precursor, which arrives at a later time, can also be detected in TOF. This enables the shot by shot normalization of technical noise associated with the precursor production. Since the scheme alters only the configuration of the high-voltage switch, it can be readily implemented in most existing gated MCP setups, allowing the full TOF information to be harvested. Combining the imaging and TOF data in a single shot, we can detect species with substantially different abundances.

Published by Elsevier Inc.

Action spectroscopy techniques, such as photoionization and photodissociation, are ubiquitous in chemical physics studies. Since these techniques alter the mass-to-charge ratio of target species, separation of the signal from the background is straightforward by time-of-flight (TOF) mass spectrometery [2]. The charged products are often detected by micro-channel plates (MCP) where quantum efficiencies as high as 80% can be achieved [3]. In contrast to dynode electron multipliers, which also have high quantum efficiency, the electrons are locally amplified in an MCP. While the electrons emitted from the back of the MCP may be guided towards an anode to extract timing information, they can also be accelerated towards a phosphor screen, which converts them into photons. By imaging this light we can extract the impact positions of the original particles. Resolving photodissociation distributions [4–8] or differential scattering cross sections [5,9–12] are common applications. In our case, we are also motivated by the signal-to-noise enhancement of counting the arrivals of distinct ions spatially spread across the detector rather than relying on an integrated signal which is subject to the large event-amplification fluctuations endemic in avalanche-based detectors.

The most common ion imaging method used in molecular scattering and spectroscopy experiments [7] is the velocity map imaging (VMI) apparatus [13]. The spatial positions of the imaged ions correspond to the initial velocities of the ions and are detected by an imaging MCP positioned at the end of a TOF tube. Since VMI also time-focuses according to the mass-to-charge ratio [13], it is beneficial to capture the image with a timing resolution of less than ~100 ns to separate the desired signal from the background. This temporal resolution is beyond the capability of most available cameras. Instead the temporal resolution is typically achieved by gating the voltage across the MCP stack, turning the electron amplification "on" only while the selected mass species impacts the MCP. One can then use cameras with modest timing capabilities. The resulting image includes only the selected mass arriving during the "MCP on" time window. Unfortunately, gating the MCP means that the remainder of the TOF trace is not amplified, wasting what may be valuable information about other ions that arrive at different times. Detection of secondary ions arriving

* Corresponding author.
E-mail address: yuval.shagam@jila.colorado.edu (Y. Shagam).
[1] Present address: Department of Chemistry and Chemical Biology, Harvard University, Cambridge, MA 02138, USA
[2] Present address: Department of Physics and Astronomy, University of Nevada, Las Vegas, Las Vegas, NV 89154, USA
[3] Present address: Honeywell Quantum Solutions 303 S Technology Ct. Broomfield, CO 80021, USA

https://doi.org/10.1016/j.jms.2020.111257
0022-2852/Published by Elsevier Inc.

outside the imaging window is useful in many instances such as signal normalization in dissociation experiments or detection of both reagents in reactive scattering, as well as for general diagnostic purposes. Here we demonstrate that the same time-selected imaging can be achieved by gating the phosphor screen as opposed to the MCP stack, while still recording TOF trace integrated on the entire MCP. While gating the phosphor screen to achieve time-selected imaging has been previously demonstrated by Zajfman et al. [1] and references therein, here we demonstrate the full benefit of this technique including the simultaneous detection of two species that may differ by more than two orders of magnitude in abundance.

In our experiment we search for the electric dipole moment of the electron [14] and the science signal is probed by spatially resolved Hf^+ photofragments [6]. The anisotropic distribution of the Hf^+ must be imaged with simultaneous monitoring of the precursor HfF^+ molecule number from the TOF trace for shot-by-shot normalization, making this gating scheme critical for our scientific purposes. We ablate Hf metal near a supersonic expansion of Ar seeded with SF_6, such that HfF is created by chemical reaction and entrained in the expansion. The HfF molecules are ionized by $1+1'$ photoionization [15] and subsequently trapped in a Paul trap. We then perform a precision spectroscopy sequence and with an efficiency contingent on the result of that sequence, the HfF^+ is dissociated by $1+1'$ photodissociation [16,14]. The resultant variable mixture of Hf^+ and HfF^+ ions is kicked out towards the imaging MCP detector located ~25 cm away to separate the species according to their mass [6].

The electron amplification depends on the voltage difference across the MCP stack [17] ($V_{back} - V_{front}$) shown in Fig. 1. This time-dependent signal (Fig. 2) integrated on the entire MCP face can be measured on the MCP stack. The output electrons from the MCP are accelerated towards the phosphor and excite it, with the luminescence of the phosphor depending on the kinetic energy ($V_{phos} - V_{back}$) of the electrons. When we lower V_{phos} to 0V the kinetic energy of the electrons falls below a certain threshold such

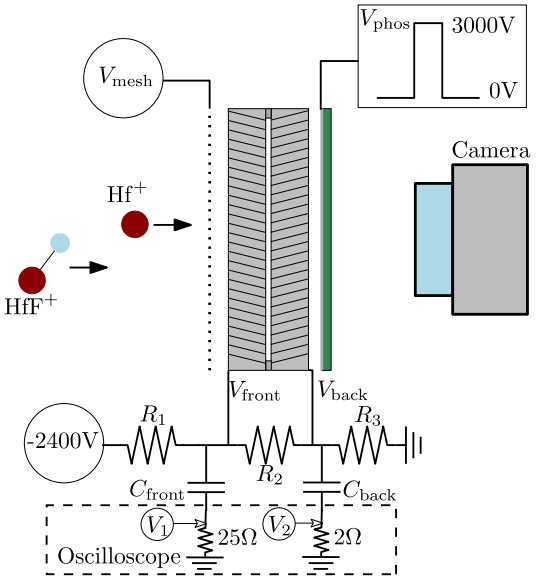

Fig. 1. Schematic diagram of the phosphor gating scheme. HfF^+ molecules and Hf^+ photofragments are accelerated towards the MCP assembly. The 2 MCPs in a "chevron" configuration are supplied by a DC voltage divider where $R_1 = 0.15$ MΩ, $R_2 = 3.2$ MΩ, and $R_3 = 1.2$ MΩ. Both the front and back of the MCPs are capacitively coupled ($C_{front} = 10$ nF, $C_{back} = 100$ nF) to an oscilloscope to measure the transient charge signals off of the MCP stack as discussed in the text. The aluminum coating on the P-43 phosphor is gated to 3000 V while the Hf^+ ions are arriving, such that this part of the signal is imaged.

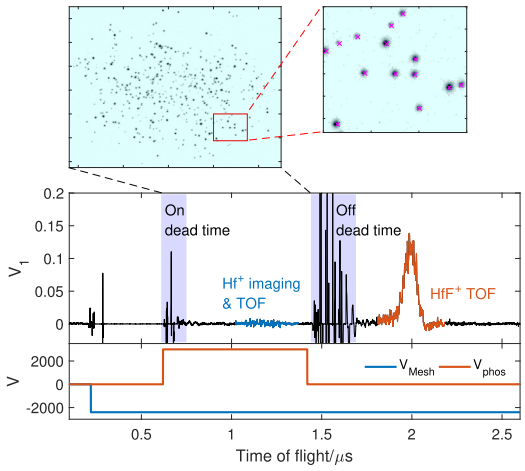

Fig. 2. Time-of-flight trace measured on the front of the MCP stack (V_1 of Fig. 1) are shown in the bottom panel. The switching of the phosphor voltage to high followed by low induces the noisy ringing shaded gray regions on the trace. The signal of Hf^+ arriving while the phosphor voltage is high is imaged by the camera (top left panel), allowing spots arising from individual ion impacts to be centroided as depicted by the magenta asterisks (top right panel). Since the MCP amplification is on even after the phosphor has been switched to low, the HfF^+ is only visible in the TOF trace from the MCP. There are 411 Hf^+ ions counted in the image and the integrated area on the TOF trace for HfF^+ corresponds to ~23,000 ions. The TOF traces and the image are acquired in the same experiment cycle.

that the multiplied electrons no longer excite the phosphor, thereby turning off the imaging. Gating V_{phos} up to 3000 V around the Hf^+ ions arrival window time-selects this portion of the signal for imaging as shown in the top panels of Fig. 2. It is critical that the electron-side face of the phosphor be conductively coated (aluminum in our case) as opposed to phosphors with indium tin oxide (ITO) coating on the opposite side, so that control of the phosphor gain is immediate. The time-scale of the excitation is much shorter than the luminescence time-scale of the phosphor (on the order of milliseconds for our P-43 phosphor), such that light emission from excited regions of the phosphor will continue. Counting of the Hf^+ is performed by applying smoothing filters to the acquired images followed by a search for local maxima and centroiding to find the ion locations (Fig. 2). In our implementation we can distinguish up to 2000 ions with image pile up of less than 10%.

Since the MCP gain is always set to high, the electron amplification is on continuously. We probe both the back and the front sides of the MCP stack through capacitors as shown in Fig. 1. These capacitors form bias tees with the high impedance voltage divider, passing the transient signal, which has a bandwidth of > 1 MHz, from the MCP plates to the scope. A full circuit analysis of the detector, including the stray capacitance through the MCP plates and a cascading electron current which amplifies as it passes through the MCP stack and eventually flows to the phosphor screen, is beyond the scope of this paper. We empirically obtain an improved dynamic range if we sample the TOF current at probe point V_1 as opposed to V_2 as shown in Fig. 3. While this added range also exhibits slight non-linearity over a larger dynamic range, we have characterized its functional form. Fig. 2 shows a single shot of data collection in which the number of dissociated Hf^+ ions is counted on the image and can be normalized by the number of undissociated HfF^+ ions determined by the integrated voltage from V_1 for the corresponding time window. This allows us to set the MCP gain and phosphor gain high enough to detect single Hf^+ events on the image, while maintaining a high dynamic range for the highly abundant HfF^+ species in the TOF traces probed on V_1.

Since the phosphor and the MCP back are capacitively coupled, the ringing noise from switching the phosphor voltage

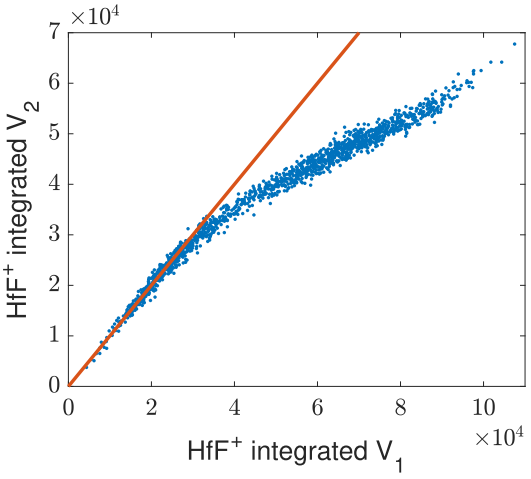

Fig. 3. Comparison of HfF^+ amounts measured simultaneously from the time-of flight traces at probe points V_1 and V_2. We observe a larger dynamic range at probe point V_1. The reliability of the V_1 measurement has been confirmed with an independent measurement.

contaminates our TOF trace. By optimizing the output impedance of the phosphor voltage switch (Behlke HTS-41-02-HB-LC-C), we were able to minimize the dead time in the TOF trace to 300 ns on the falling edge such that the trace is quiet before the HfF^+ arrives. A background trace measuring the electronic noise due to the switching is subtracted from the TOF trace in Fig. 2.

In our particular application, a fine grounding mesh (Fig. 1) is used in front of the MCP to reduce the effect of the MCP's electric fields on other parts of our apparatus. The presence of this mesh comes at a cost – the intense fields near the fine wires give rise to ion focusing in the grid spaces aggravating our ion-image pileup. This so-called microlensing can be avoided by gating the mesh voltage to equal V_{front} before the arrival of the ions (Fig. 2). The electrical noise impact of gating a separate mesh on the temporal signals is significantly smaller than if V_{front} was gated, due to the low capacitive and vanishing resistive coupling between V_{mesh} and probe points V_1 and V_2.

As an alternative to the technical solution presented in this paper, one could achieve the desired spatial and temporal detection using some combination of various other options: delay-line detectors [18]; anode arrays [19]; individually triggered camera pixels [20,21]; gated image intensifiers [22]. Some of these approaches are more vulnerable to event pile-up [18,19] and moreover they all tend to require more financial resources than does our approach.

In summary, we have shown that if we gate the phosphor instead of the MCP stack, time-gated imaging can be achieved while simultaneously measuring nearly all of the TOF signal. Although this was not our goal here, it may be possible to achieve shorter image gating windows than in schemes that switch the voltage on the MCP, due to the much lower capacitance of the phosphor screen, which is on the order of ~10 pF.

Author contribution

All authors contributed to all aspects of this work.

Declaration of Competing Interest

The authors declare that they have no known competing financial interests or personal relationships that could have appeared to influence the work reported in this paper.

Acknowledgement

We thank T. Brown for fruitful discussions. Y.S. is supported by a postdoctoral fellowship from the National Research Council. Commercial products referenced in this work are not endorsed by NIST and are for the purposes of technical communication only. This work was supported by the Marsico Foundation, NIST, and the NSF (Grant No. PHY-1734006).

References

[1] D. Zajfman, Z. Amitay, C. Broude, P. Forck, B. Seidel, M. Grieser, D. Habs, D. Schwalm, A. Wolf, Measurement of branching ratios for the dissociative recombination of cold HD+ using fragment imaging, Phys. Rev. Lett. 75 (1995) 814–817, https://doi.org/10.1103/PhysRevLett. 75.814.
[2] W.C. Wiley, I.H. McLaren, Time–of–flight mass spectrometer with improved resolution, Rev. Sci. Instrum. 26 (12) (1955) 1150–1157, https://doi.org/10.1063/1.1715212.
[3] K. Fehre, D. Trojanowskaja, J. Gatzke, M. Kunitski, F. Trinter, S. Zeller, L.P.H. Schmidt, J. Stohner, R. Berger, A. Czasch, O. Jagutzki, T. Jahnke, R. Dörner, M.S. Schöffler, Absolute ion detection efficiencies of microchannel plates and funnel microchannel plates for multi-coincidence detection, Rev. Sci. Instrum. 89 (4) (2018), https://doi.org/10.1063/1.5022564. 045112.
[4] D.W. Chandler, P.L. Houston, Two-dimensional imaging of state-selected photodissociation products detected by multiphoton ionization, J. Chem. Phys. 87 (2) (1987) 1445–1447, https://doi.org/10.1063/1.453276.
[5] M.N.R. Ashfold, N.H. Nahler, A.J. Orr-Ewing, O.P.J. Vieuxmaire, R.L. Toomes, T.N. Kitsopoulos, I.A. Garcia, D.A. Chestakov, S.-M. Wu, D.H. Parker, Imaging the dynamics of gas phase reactions, Phys. Chem. Chem. Phys. 8 (2006) 26–53, https://doi.org/10.1039/B509304J.
[6] Y. Zhou, Y. Shagam, W.B. Cairncross, K.B. Ng, T.S. Roussy, T. Grogan, K. Boyce, A. Vigil, M. Pettine, T. Zelevinsky, J. Ye, E.A. Cornell, Second-scale coherence measured at the quantum projection noise limit with hundreds of molecular ions, Phys. Rev. Lett. 124 (5) (2020) 53201, https://doi.org/10.1103/PhysRevLett.124.053201.
[7] D.W. Chandler, P.L. Houston, D.H. Parker, Perspective: advanced particle imaging, J. Chem. Phys. 147 (1) (2017), https://doi.org/10.1063/1.4983623. 013601.
[8] T. Suzuki, H. Katayanagi, Y. Mo, K. Tonokura, Evidence for multiple dissociation components and orbital alignment in 205 nm photodissociation of N2O, Chem. Phys. Lett. 256 (1) (1996) 90–95, https://doi.org/10.1016/0009-2614(96)00429-0.
[9] R.T. Skodje, D. Skouteris, D.E. Manolopoulos, S.-H. Lee, F. Dong, K. Liu, Resonance-mediated chemical reaction: F+HD→HF+D, Phys. Rev. Lett. 85 (2000) 1206–1209, https://doi.org/10.1103/PhysRevLett. 85.1206.
[10] D. Yuan, Y. Guan, W. Chen, H. Zhao, S. Yu, C. Luo, Y. Tan, T. Xie, X. Wang, Z. Sun, D.H. Zhang, X. Yang, Observation of the geometric phase effect in the H + HD H2 + D reaction, Science 362 (6420) (2018) 1289–1293, https://doi.org/10.1126/science.aav1356.
[11] J. Mikosch, S. Trippel, C. Eichhorn, R. Otto, U. Lourderaj, J.X. Zhang, W.L. Hase, M. Weidemüller, R. Wester, Imaging nucleophilic substitution dynamics., Science (New York, N.Y.) (5860) 183–6. doi:https://doi.org/10.1126/science.1150238.
[12] S.N. Vogels, J. Onvlee, S. Chefdeville, A. van der Avoird, G.C. Groenenboom, S.Y.T. van de Meerakker, Imaging resonances in low-energy NO-He inelastic collisions., Science (New York, N.Y.) (6262) 787–90. doi:https://doi.org/10.1126/science.aad2356.
[13] A.T.J.B. Eppink, D.H. Parker, Velocity map imaging of ions and electrons using electrostatic lenses: Application in photoelectron and photofragment ion imaging of molecular oxygen, Rev. Sci. Instrum. 68 (9) (1997) 3477–3484, https://doi.org/10.1063/1.1148310.
[14] W.B. Cairncross, D.N. Gresh, M. Grau, K.C. Cossel, T.S. Roussy, Y. Ni, Y. Zhou, J. Ye, E.A. Cornell, Precision measurement of the electron's electric dipole moment using trapped molecular ions, Phys. Rev. Lett. 119 (2017), https://doi.org/10.1103/PhysRevLett. 119.153001. 153001.
[15] H. Loh, R.P. Stutz, T.S. Yahn, H. Looser, R.W. Field, E.A. Cornell, REMPI spectroscopy of HfF, J. Mol. Spectrosc. 276–277 (2012) 49–56, https://doi.org/10.1016/j.jms.2012.06.014.
[16] K.-K. Ni, H. Loh, M. Grau, K.C. Cossel, J. Ye, E.A. Cornell, State-specific detection of trapped HfF^+ by photodissociation, J. Mol. Spectrosc. 300 (2014) 12–15, https://doi.org/10.1016/j.jms.2014.02.001. spectroscopic Tests of Fundamental Physics.
[17] E.H. Eberhardt, Gain model for microchannel plates, Appl. Opt. 18 (9) (1979) 1418–1423, https://doi.org/10.1364/AO.18.001418.
[18] O. Jagutzki, V. Mergel, K. Ullmann-Pfleger, L. Spielberger, U. Spillmann, R. Dörner, H. Schmidt-Böcking, A broad-application microchannel-plate detector system for advanced particle or photon detection tasks: large area imaging, precise multi-hit timing information and high detection rate, Nucl. Instrum. Meth. Phys. Res. Section A: Acceler. Spectrometers Detectors Assoc. Equip. 477 (1) (2002) 244–249, 5th Int. Conf. on Position-Sensitive Detectors.
[19] J.G. Timothy, Review of multianode microchannel array detector systems, J. Astronom. Telescopes Instrum. Syst. 2 (3) (2016) 030901, https://doi.org/10.1117/1.JATIS.2.3.030901.

[20] M. Brouard, E. Halford, A. Lauer, C.S. Slater, B. Winter, W.H. Yuen, J.J. John, L. Hill, A. Nomerotski, A. Clark, J. Crooks, I. Sedgwick, R. Turchetta, J.W.L. Lee, C. Vallance, E. Wilman, The application of the fast, multi-hit, pixel imaging mass spectrometry sensor to spatial imaging mass spectrometry, Rev. Sci. Instrum. 83 (11) (2012), https://doi.org/10.1063/1.4766938. 114101.
[21] M. Fisher-Levine, A. Nomerotski, TimepixCam: a fast optical imager with time-stamping, J. Instrum. 11 (03) (2016), https://doi.org/10.1088/1748-0221/11/03/c03016. C03016–C03016.
[22] D. Strasser, X. Urbain, H.B. Pedersen, N. Altstein, O. Heber, R. Wester, K.G. Bhushan, D. Zajfman, An innovative approach to multiparticle three-dimensional imaging, Rev. Sci. Instrum. 71 (8) (2000) 3092–3098, https://doi.org/10.1063/1.1305514.